Howard Hughes Medical Institute

Published as: *J Am Chem Soc*. 2018 May 30; 140(21): 6596–6603.

Receptor-Mediated Delivery of CRISPR-Cas9 Endonuclease for Cell-Type-Specific Gene Editing

Romain Rouet[†,‡], **Benjamin A. Thuma**[§], **Marc D. Roy**[||], **Nathanael G. Lintner**[⊥], **David M. Rubitski**[||], **James E. Finley**[||], **Hanna M. Wisniewska**[§], **Rima Mendonsa**[‡,&], **Ariana Hirsh**[‡,&], **Lorena de Oñate**[‡,&], **Joan Compte Barrón**[‡,&], **Thomas J. McLellan**[§], **Justin Bellenger**[§], **Xidong Feng**[§], **Alison Varghese**[§], **Boris A. Chrunyk**[§], **Kris Borzilleri**[§], **Kevin D. Hesp**[§], **Kaihong Zhou**[†,‡], **Nannan Ma**[†,‡], **Meihua Tu**[⊥], **Robert Dullea**[#], **Kim F. McClure**[⊥], **Ross C. Wilson**[‡,&], **Spiros Liras**[⊥,*,∞], **Vincent Mascitti**[§,*,×], and **Jennifer A. Doudna**[†,‡,⊗,▽,&,%,*,×,∞]

[†]Department of Molecular and Cell Biology, University of California, Berkeley, California 94720, United States

[‡]California Institute for Quantitative Biosciences, University of California, Berkeley, California 94720, United States

[⊗]Howard Hughes Medical Institute, University of California, Berkeley, California 94720, United States

[▽]Department of Chemistry, University of California, Berkeley, California 94720, United States

[&]Innovative Genomics Institute, University of California, Berkeley, California 94720, United States

[§]Pfizer Medicine Design, Groton, Connecticut 06340, United States

[||]Pfizer Drug Safety R&D, Groton, Connecticut 06340, United States

[⊥]Pfizer Medicine Design, Cambridge, Massachusetts 02139, United States

[#]Pfizer CVMET Biology, Cambridge, Massachusetts 02139, United States

[*]Corresponding Authors: spiros.liras@pfizer.com, vincent.mascitti@pfizer.com, doudna@berkeley.edu.
[×]Research project leaders.
[∞]Collaboration leaders.

ORCID

Alison Varghese: 0000-0001-8708-0135
Ross C. Wilson: 0000-0002-0644-5540
Jennifer A. Doudna: 0000-0001-9161-999X

Notes

The authors declare the following competing financial interest(s): S.L., V.M., B.A.T., J.A.D., and R.R. have filed intellectual property protection on tissue-specific genome engineering using CRISPR-Cas9 (U.S. Patent Application No. 62/254,652; WO2017/083368). J.A.D. is employed by HHMI and works at the University at California, Berkeley. UC Berkeley and HHMI have patents pending for CRISPR technologies on which she is an inventor. J.A.D. is the executive director of the Innovative Genomics Institute at UC Berkeley and UCSF. J.A.D. is a co-founder of Editas Medicine, Intellia Therapeutics, Mammoth Biosciences, Caribou Biosciences, and Scribe Therapeutics; a scientific advisor to Caribou, Intellia, Scribe, eFFECTOR Therapeutics, Inari, Synthego, and Metagenomi; and a board member of Driver and Johnson & Johnson. All authors, except Barrón, de Oñate, Doudna, Hirsh, Ma, Mendonsa, Rouet, Wilson, and Zhou, were employed by Pfizer, Inc. at the time this work was done.

Supporting Information

The Supporting Information is available free of charge on the ACS Publications website at DOI: 10.1021/jacs.8b01551.
Information related to synthesis, conjugation, purification, and additional experimental and analytical details; Figures S1–S19, Tables S1–S6; custom script for data analysis (PDF)

[%]MBIB Division, Lawrence Berkeley National Laboratory, Berkeley, California 94720, United States

Abstract

CRISPR-Cas RNA-guided endonucleases hold great promise for disrupting or correcting genomic sequences through site-specific DNA cleavage and repair. However, the lack of methods for cell- and tissue-selective delivery currently limits both research and clinical uses of these enzymes. We report the design and in vitro evaluation of *S. pyogenes* Cas9 proteins harboring asialoglycoprotein receptor ligands (ASGPrL). In particular, we demonstrate that the resulting ribonucleoproteins (Cas9-ASGPrL RNP) can be engineered to be preferentially internalized into cells expressing the corresponding receptor on their surface. Uptake of such fluorescently labeled proteins in liver-derived cell lines HEPG2 (ASGPr+) and SKHEP (control; diminished ASGPr) was studied by live cell imaging and demonstrates increased accumulation of Cas9-ASGPrL RNP in HEPG2 cells as a result of effective ASGPr-mediated endocytosis. When uptake occurred in the presence of a peptide with endosomolytic properties, we observed receptor-facilitated and cell-type specific gene editing that did not rely on electroporation or the use of transfection reagents. Overall, these in vitro results validate the receptor-mediated delivery of genome-editing enzymes as an approach for cell-selective gene editing and provide a framework for future potential applications to hepatoselective gene editing in vivo.

Graphical Abstract

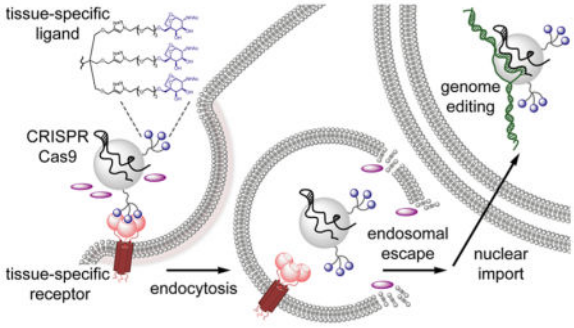

INTRODUCTION

CRISPR-Cas9 RNA-guided endonucleases are efficient and versatile tools for genome editing.[1,2] After a Cas9 ribonucleoprotein (RNP) catalyzes site-specific genomic DNA cleavage, endogenous repair at the targeted site leads to gene disruption or templated repair that can correct the underlying cause of genetic disorders. To date, this technology has been successfully employed in both cultured cells and animals to edit genes responsible for diseases such as hereditary tyrosinemia type I,[3] hypercholesterolemia,[4] β-hemoglobinopathy[5,6] and muscular dystrophy.[7] As for any genome engineering technology, selectivity is of paramount importance and identifying avenues for cell-type specific delivery presents tremendous opportunities to advance the application of Cas9-guide RNA complexes for safe somatic genome editing.[8] To address the need for targeted delivery methods of Cas9-guide RNA complexes, we investigated whether known receptor–ligand interactions

can be harnessed for tissue-specific Cas9 RNP uptake and gene editing. This approach would allow receptor-facilitated, cell-selective, gene editing without the concerns associated with the delivery of foreign genetic material using viruses or nanoparticles. Current delivery methods include plasmid- and virus-based vectors encoding Cas9 and guide RNAs,[4,5,7] as well as delivery of guide RNA and Cas9 in the form of protein[9] or mRNA,[10–12] respectively facilitated by cationic peptides or nanoparticles. Successful delivery of preassembled RNP has also been accomplished using nanoparticle encapsulation[13–15] or via direct injection.[16] Although some viral vectors have tissue-specific tropism,[17] their use presents risks of insertional mutagenesis, liver toxicity, and immunogenicity.[18–20] Potential for off-target editing due to prolonged Cas9 and guide RNA expression is also a concern.[8,21] Direct or nanoparticle-based delivery of Cas9-guide RNA RNP complexes can substantially decrease off-target risks[22] but has not yet been developed for tissue-specific uptake. Cas9 RNPs have also been delivered to mammalian cell lines by electroporation,[23] chemical transfection,[15] or using DNA nanoclews,[24] but these methods are not suitable for the treatment of animals or humans.

We focused our initial efforts on cell-specific delivery to cells of hepatic origin as many metabolic, cardiovascular, and rare diseases could, in principle, be treated by selective hepatocyte gene editing. With these possibilities in mind, we chose to utilize the asialoglycoprotein receptor (ASGPr), a C-type lectin of very high capacity expressed almost exclusively on the surface of hepatocytes.[25] ASGPr is involved in the homeostasis of proteins containing galactose and *N*-acetylgalactosamine (GalNAc) epitopes such as the 40 kDa glycoprotein asialoorosomucoid (ASOR).[26] This receptor has also been used for the delivery of oligonucleotide therapeutics to the liver.[27–30] We reasoned that by engineering Cas9 RNPs harboring ASGPr ligands (Cas9-ASGPrL RNP) one could promote, via a receptor-mediated endocytosis mechanism, the selective uptake of this cargo into cells expressing ASGPr on their surface (Figure 1A). An analogous strategy has been employed for transferrin-mediated delivery of zinc finger nucleases engineered for genome editing.[31] In our strategy, acidification in the early endosome would trigger the release of the ASGPr ligand from the receptor accompanied by recycling of the receptor at the cell surface. Critical to the success of this approach would be the ability to not only internalize a large cargo like a Cas9-ASGPrL RNP (~170 kDa) but also promote its endosomal escape to avoid subsequent lysosomal degradation. Indeed, endosomal escape is currently a major hurdle to the delivery of any therapeutic macromolecule via receptor mediated endocytosis, including antisense oligonucleotides and small interfering RNAs.[32] Existing strategies for delivery of genome-editing enzymes have employed membrane-disrupting cationic peptides to facilitate cellular entry,[33] which can unfortunately also lead to nonselective uptake. To circumvent this issue, we envisioned the need of an endosomolytic agent (i.e., a compound that would selectively disrupt the endosomal membrane and not perturb the cellular membrane) to promote endosomal escape of the RNP cargo to the cytosol. Subsequent entry to the nucleus would be mediated by a nuclear localization sequence (NLS) fused to Cas9, ultimately promoting gene editing. Overall, by achieving receptor-facilitated, cell-selective, gene editing without the concerns associated with the delivery of foreign genetic material, this approach would also establish a new paradigm for cellular delivery of genome-editing enzymes.

RESULTS AND DISCUSSION

Recently, we reported the discovery of a novel ASGPr ligand (receptor K_D = 7 μM).[34] Trimers thereof (receptor K_D ≤100 pM) led to superior ASGPr-mediated hepatocellular uptake compared to similar GalNAc trimers and have been used for the hepatoselective delivery of small molecule modulators of the glucocorticoid receptor in vivo. Building on this finding, we focused our initial efforts at developing a method to regio- and chemoselectively ligate trimeric displays of this ASGPr ligand (ASGPrL) to the genome-editing enzyme Cas9. To this end, we designed pyridyl disulfide-activated ASGPr ligand molecules **1** and **3** as candidates for ligation via disulfide bond formation with solvent-exposed cysteines of the protein (Figure 1B). To facilitate preliminary live cell-imaging studies, we used a *Streptococcus pyogenes* (*Sp*) Cas9M1C/C80S mutant (bearing two cysteines, including the native C574), fused at its C-terminus with the mCherry fluorescent protein and harboring three nuclear localization sequences derived from SV40 (henceforth Cas9-mCh). These solvent-exposed cysteine sites were selected based on their strong activity in conjugation reactions, as opposed to the native site at residue 80, which was mutated to serine to prevent side reactions (C80 is located in an area critical for sgRNA binding). Treatment of Cas9-mCh with **1** resulted in a bis-ligated protein, Cas9-2lig-mCh, as confirmed by mass spectrometry (Figure S1A). Functional activity was evaluated in vitro by nucleofection of the corresponding RNP enzyme (Cas9-2lig-mCh bound to a sgRNA targeting the EMX1 gene) into HEPG2 cells, a human hepatocarcinoma cell line that expresses ASGPr,[26,34] and assessing gene editing after 48 h of incubation (see the Supporting Information). The T7E1 endonuclease cleavage assay qualitatively showed levels of editing similar to that obtained with the ligand-free RNP equivalent (as observed by gel electrophoresis; see Figure S1B). Next, we investigated the ability of Cas9-2lig-mCh RNP to bind to ASGPr. Surface plasmon resonance measurements revealed a binding affinity (K_D) of 92 pM for the bis-ligated RNP while the unligated equivalent did not bind the receptor (Figure 1C; Figure S1C,D). The monoligated Cas9-1lig-mCherry (generated using Sp Cas9 C80S mutant fused with mCherry) had a weaker affinity of 920 ± 18 pM (n = 3) and prompted us to use the bisligated construct in our subsequent studies. Thus, CRISPR-Cas endonucleases can be engineered by regio- and chemoselective chemical conjugation of ASGPrL for highly effective binding to ASGPr without negatively impacting the RNP's endonuclease activity.

To test the hypothesis that large cargoes like Cas9-ASGPrL RNPs could be endocytosed via ASGPr, we compared the uptake of the Cas9-2lig-mCh and Cas9-mCh RNPs by live cell imaging in HEPG2 (ASGPr expressing) and SKHEP (ASGPr diminished; control) cells. HEPG2 cells have less ASGPr expressed on their surface than primary hepatocytes (~76000 vs 500000, respectively) but express far more than SKHEP cells, and as such, the tandem HEPG2/SKHEP cell is a standard and validated in vitro model to study ASGPr-mediated mechanisms of uptake.[35,36] They also present the practical advantage of being easier to handle than primary hepatocytes, which are known to be prone to readily lose their phenotype in vitro.[37] Increased uptake and intracellular accumulation was observed for the ligated versus the unligated construct at early time points (e.g., 7-fold increase at 1.5 h, Figure 2; also see Figure S2) with some cell surface accumulation also apparent for the

unligated Cas9-mCh RNP (Figures S2 and S3). Interestingly, at later time points, uptake of the unligated RNP resulted in a reduction of the uptake enhancement initially observed for the ligated RNP (3- and 0-fold increase at 4 and 20 h, respectively). For both constructs, fluorescence was localized in endolysosomal vesicles, and colocalization with endolysosomes was observed over time (Figure 2), although the ligated construct was taken up more readily at 1 h (Figure 2 and Figure S2). To a lesser extent, accumulation was also detected for both constructs in SKHEP cells (Figure S4). A ligand competition assay using ASGPr ligand **4** (K_D = 369.9 ± 0.4 pM) and Cas9-2lig-mCh RNP in HEPG2 cells revealed only a modest decrease in uptake of the RNP as the amount of competing ligand increased (Figure 2D; see also Figure S11). Together, these results demonstrate that the Cas9-2lig-mCh RNP is capable of ASGPr-mediated endocytosis; however, upon prolonged exposure in vitro in a medium containing HEPG2 or SKHEP cells, these Cas9-mCh RNPs appear capable of entering cells nonspecifically via ASGPr-independent mechanism(s) of active and/or passive uptake. Such alternative uptake pathways may be dependent on, or at least enhanced by, the multiple NLS regions of these Cas9 constructs. As previously reported, the positively charged residues of such sequences could contribute to nonspecific interactions with the negatively charged mammalian cell membrane, leading to the cell surface accumulation observed at early time points (Figures S2 and S3), and ultimately promote nonspecific uptake.[16,38,39] The variability observed for the sum fluorescence intensity per cell with the Cas9-mCh in HEPG2 cells may be due to the various uptake mechanisms at play with this construct (Figure 2C).

As a result of these findings, we focused subsequent efforts on optimizing the selectivity for ASGPr-mediated uptake over other possible mechanisms of entry into the cell. Observations from live cell imaging with the Cas9-2lig-mCh suggested that the design of a construct with fewer NLS and lacking the mCherry fusion may be a productive strategy moving forward. Furthermore, previous work has demonstrated that multiple NLS are not necessary for nuclear import in cultured cells.[16,40]

Disulfide exchange between pyridyl disulfide activated ASGPrL **1** and *Sp* Cas9M1C/C80S mutant (containing two cysteines, including the native C574) and bearing a single SV40 NLS at the C-terminus (Cas9-1NLS) provided the corresponding bis-ligated Cas9-2lig-1NLS. Mass spectrometry following protein digestion unambiguously confirmed ligation at residues C1 and C574 (Figure S5). The corresponding RNP (Cas9-2lig-1NLS bound to sgRNA targeting the EMX1 gene) showed high binding affinity for ASGPr with a K_D of 47 pM (Figure 1C, Figure S6A) and retained functional activity under nucleofection conditions as measured by deep sequencing (22.1 [ligated] vs 25.4 [unligated] % indels; Table S1 and Figure S6B,C). Of note, the deep sequencing utilized a library incorporating unique molecular identifier (UMI) tags to avoid any PCR amplification bias (see the Supporting Information). Cas9-2lig-1NLS RNP resulted in a 7-fold increase in binding affinity compared to compound **4**. This can be rationalized by the well-known avidity "cluster glycoside" effect where the RNP has more ASGPr ligand monomers than **4** (6 vs 3).[41,42] To compare the uptake of this new construct with its unligated 1NLS progenitor via live cell imaging, we made the fluorescently labeled proteins Cas9-AFr-1NLS and Cas9-2lig-AFr-1NLS; these proteins were respectively made via disulfide exchange using linker **2** and

branched linker **3**, which harbors both the red Alexa Fluor 647 (AF647, AFr) dye and the ASGPrL (Figure 1B). As expected, the RNPs derived from these two proteins were shown to retain endonuclease activity under nucleofection (Figure S6D), and Cas9-2lig-AFr-1NLS RNP had a K_D similar to Cas9-2lig-1NLS RNP, whereas Cas9-AFr-1NLS RNP did not bind to ASGPr (Figure 1C). Cas9-2lig-AFr-1NLS RNP showed substantially increased uptake (e.g., 9-fold increase at 4 h) compared to Cas9-AFr-1NLS RNP as measured by the sum fluorescence intensity per HEPG2 cell over time (Figure 3). Furthermore, superior intracellular accumulation of the ligated species was maintained over time (Figure 3C), and minimal cell surface accumulation was observed (Figure S7). The comparatively weaker and linear uptake in HEPG2 of the RNP lacking ASGPrL is likely due to non-ASGPr-mediated uptake occurring over time in vitro; indeed, similar low levels of linear uptake were also observed for both RNP constructs in SKHEP cells (Figure 3D; Figure S8). The same trends were observed when the sum fluorescence intensity in endolysosomes was monitored over time (Figure S9). A ligand competition assay using ASGPr ligand **4** and HEPG2 cells revealed a clear dose-responsive decrease in uptake of the Cas9-2lig-AFr-1NLS RNP as the amount of competing ligand increased (Figure 4A). In addition, the competing ligand was observed to have no effect on uptake of the Cas9-AFr-1NLS RNP into HEPG2 cells (Figure 4A) or when SKHEP cells were incubated with either of the two AF647-labeled RNPs (Figure S10). Interestingly, the use of 100 equiv of competing ASGPr ligand **4** almost completely inhibited the uptake of the Cas9-2lig-AFr-1NLS RNP in HEPG2 cells (29-fold decrease) at 3 h, whereas a similar competition experiment using Cas9-2lig-mCh RNP resulted in only comparatively modest uptake inhibition (2-fold decrease; Figure S11). This is consistent with additional NLS (compared to Cas9-1NLS constructs) and mCherry fusion contributing to non-ASGPr mediated uptake pathway(s) of the Cas9-2lig-mCh RNP in HEPG2 cells. Observation of the uptake of a differently labeled construct, AFg-Cas9-2lig-1NLS RNP, via monitoring internalized green AF532 (AFg) fluorescence also confirmed drastically increased accumulation in HEPG2 compared to SKHEP cells (Figure S12). AFg-Cas9-2lig-1NLS RNP construct was derived from Cas9-2lig-1NLS by covalent linkage of two AF532 to the protein via amide bond formation to solvent-exposed lysines (average degree of ligation as determined by mass spectrometry: 2.3.) All these results demonstrate that the uptake of Cas9-2lig-1NLS RNP in HEPG2 cells is ASGPr-mediated and follows an endocytotic/lysosomal pathway. Live cell imaging using a doubly labeled AF532/AF647 RNP, AFg-Cas9-2lig-AFr-1NLS, derived from Cas9-2lig-AFr-1NLS confirmed that the entire cargo (linker+protein) is internalized and colocalized in endocytotic vesicles (Figure S13). AF532 was covalently linked to solvent-exposed lysines via amide bond formation (average degree of ligation as determined by mass spectrometry: 1.7.)

While the above studies confirmed the ASGPr-mediated uptake of Cas9-2lig-1NLS RNP in HEPG2 cells, upon incubation for 48 h only nominal functional activity was detected by T7E1 assay or deep sequencing (Table S1). After ruling out that early endosomal pH levels might abrogate RNP function (Figure S14), we hypothesized that the RNP is endocytosed but unable to escape the endosome and may be degraded via the lysosomal pathway. We therefore screened candidate endosomolytic agents with an emphasis on identifying a compound with a pI between 7 and 8 and close to neutrally charged at physiological pH to

avoid agents that would be generally cell penetrating and thereby jeopardizing selectivity.[32,43–45] These efforts led to the identification of peptide ppTG21[46] (GLFHALLHLLHSLWHLLLHA-OH; Figure S15) as a promising endosomolytic agent (pI 7.7, charge +1.3 @ pH 7.4). Indeed, while only nominal editing was observed upon Cas9-2lig-1NLS RNP incubation in either HEPG2 or SKHEP cells, gene editing was observed upon coincubation of the RNP in the presence of 30 molar equiv of ppTG21 salt (4.8% indels, Figure 4B; see also Table S1 and Figure S16A). Of importance, the gene editing observed in HEPG2 cells was close to 10 times greater than that performed by the ligand-free Cas9-1NLS RNP co-incubated with ppTG21 (0.5% indels).[47] Negligible editing was observed for either construct in SKHEP cells under co-incubation conditions with ppTG21 (Table S1 and Figure S16C). Thus, we have developed a ligand-conjugated ribonucleoprotein that is taken up in a highly preferential manner by cells that bear the cognate receptor and that is conducive to receptor-facilitated, cell-selective gene editing in vitro.

Based on the knowledge that primary human hepatocytes bear substantially more surface ASGPr than HEPG2[36] and the recent report that some macromolecular therapeutics promote the expected pharmacological response following ASGPr-mediated delivery into primary murine hepatocytes but not into HEPG2 cells,[30] we tested RNP uptake and ppTG21-facilitated genome editing using primary human hepatocytes (see the Supporting Information). Fluorescent microscopy revealed robust uptake of Cas9-2lig-AFr-1NLS (Figure S17). However, preliminary RNP coincubation with ppTG21 did not result in detectable gene editing (Figures S18 and S19), suggesting that additional optimization, of endosomal escape in particular, will be needed for editing of primary hepatocytes. Future work will also investigate the feasibility of enabling this platform in vivo, which could potentially be hampered by dilution of the endosomolytic peptide in systemic circulation. To this end, preliminary experiments revealed that there appears to be strong noncovalent binding of the peptide to the RNP, suggesting that the coincubation strategy described herein may be a viable approach for potential future in vivo applications (see Tables S2–S4). Beyond endosomal escape and pharmacodynamic considerations, the in vivo clearance, distribution, and tolerability of the Cas9-ASGPrL RNP would also need to be studied to fully assess its therapeutic potential. Immunogenicity of bacterially derived Cas9 is a potential concern,[48] although use of Cas9 RNP has been proposed as an attractive alternative to other delivery methods.[49] Promisingly, a recent study delivered RNP in mice using gold-based nanoparticles and repeat administration showed no immunogenic response based on inflammatory cytokines.[13]

CONCLUSIONS

Gene editing using CRISPR-Cas9 holds great promise for therapeutic use if safe and effective methods of selectively delivering editing molecules into tissues of interest can be developed. Here, we present the reduction to practice in vitro of an approach to receptor-facilitated and cell-type selective gene editing. Focusing on hepatocyte-selective delivery, an engineered CRISPR-Cas9 RNA-protein complex (RNP) harboring a ligand for the ASGPr, a receptor expressed almost exclusively by liver-derived cells (e.g., HEPG2), was shown to be internalized via receptor-mediated endocytosis. Subsequent endosomal escape, assisted by

an endosomolytic agent, followed by nuclear transport, ultimately resulted in selective gene editing. We found that uptake efficiencies and outcomes varied depending on the nature of the RNP construct, demonstrating the nuanced impacts of varying molecular components. These experiments also revealed that endosomal escape remains a bottleneck in this approach, underscoring the value of continued development of endosomolytic agents that can be used with RNPs to help further increase gene editing efficiency and enable future in vivo experiments. Receptormediated and cell-type specific delivery of a genome-editing enzyme such as Cas9 may embody attractive properties in contrast to other platforms, including the potential for small particle sizes that evade liver filtration and are unattainable with delivery of mRNA, finite and localized of the host to the active enzyme (which cannot be guaranteed with viral delivery approaches), and compatibility with base editor strategies capable of sequence correction without inducing genomic DNA cleavage. Overall with this work, we have established a potentially generalizable strategy for receptor-mediated uptake of RNP complexes, and we are optimistic that such an approach may eventually allow in vivo delivery of genome-editing enzymes to targeted cell types.

MATERIALS AND METHODS

Details of the materials and methods used in this study are provided in the Supporting Information. Briefly, Cas9 protein constructs were purified via methods adapted from a previous report,[1] and EMX-targeting sgRNAs were synthesized via in vitro transcription using a dual-ribozyme strategy to produce homogeneous termini. Cas9 protein constructs were ligated to dendrimers of an ASGPr ligand[34] via disulfide exchange and subjected to additional purification. Microscopy was performed using cells plated onto gelatin-coated 96-well plates using an Operetta CLS confocal imager (PerkinElmer). Each genome editing experiment was performed using 80000 cells in a gelatin-coated well of a 24-well plate, incubated with 250 pmol RNP (and 7.5 nmol ppTG21 salt for coincubations), with genomic DNA harvested after 44–48 h. Next-generation sequencing utilized unique molecular identifier (UMI) tags and heterogeneity tags and was run using Illumina MiniSeq or NextSeq instruments.

Supplementary Material

Refer to Web version on PubMed Central for supplementary material.

Acknowledgments

R.R. thanks A. Iavarone and the QB3/Chemistry Mass Spectrometry Facility for native mass spectrometry analyses, A. Tambe and S. Floor for analysis discussions, and B. Staahl, C. Fellman, and other members of the Doudna lab for helpful support and discussions. This work was supported by grants from Pfizer Worldwide Research & Development (Fund 86059). R.R. acknowledges support from the Australian National Health and Medical Research Council for his early career postdoctoral fellowship (APP1090875). The Pfizer coauthors thank Dr. Chris Limberakis for sourcing of ppTG21, Greg Ciszewski for assistance with purification of compounds **1**–**4**, Wen Lin for assistance with synthesis of **3**, Steve Kumpf for assistance with deep sequencing, and Dr. Santos Carvajal-Gonzalez for statistical analysis of the data. J.A.D. is an investigator of the Howard Hughes Medical Institute. This article is dedicated to Professor E.J. Corey on the occasion of his 90th birthday and for his many contributions to chemistry.

References

1. Jinek M, Chylinski K, Fonfara I, Hauer M, Doudna JA, Charpentier E. Science. 2012; 337(6096): 816–821. [PubMed: 22745249]
2. Fellmann C, Gowen BG, Lin PC, Doudna JA, Corn JE. Nat Rev Drug Discovery. 2017; 16(2):89–100. [PubMed: 28008168]
3. Yin H, Xue W, Chen S, Bogorad RL, Benedetti E, Grompe M, Koteliansky V, Sharp PA, Jacks T, Anderson DG. Nat Biotechnol. 2014; 32(6):551–553. [PubMed: 24681508]
4. Ding Q, Strong A, Patel KM, Ng SL, Gosis BS, Regan SN, Cowan CA, Rader DJ, Musunuru K. Circ Res. 2014; 115(5):488–492. [PubMed: 24916110]
5. Traxler EA, Yao Y, Wang YD, Woodard KJ, Kurita R, Nakamura Y, Hughes JR, Hardison RC, Blobel GA, Li C, et al. Nat Med. 2016; 22(9):987–990. [PubMed: 27525524]
6. Dever DP, Bak RO, Reinisch A, Camarena J, Washington G, Nicolas CE, Pavel-Dinu M, Saxena N, Wilkens AB, Mantri S, et al. Nature. 2016; 539(7629):384–389. [PubMed: 27820943]
7. Long C, Amoasii L, Mireault AA, McAnally JR, Li H, Sanchez-Ortiz E, Bhattacharyya S, Shelton JM, Bassel-Duby R, Olson EN. Science. 2016; 351(6271):400–403. [PubMed: 26721683]
8. Tycko J, Myer VE, Hsu PD. Mol Cell. 2016; 63(3):355–370. [PubMed: 27494557]
9. Ramakrishna S, Kwaku Dad A-B, Beloor J, Gopalappa R, Lee S-K, Kim H. Genome Res. 2014; 24(6):1020–1027. [PubMed: 24696462]
10. Yin H, Song C-Q, Suresh S, Wu Q, Walsh S, Rhym LH, Mintzer E, Bolukbasi MF, Zhu LJ, Kauffman K, et al. Nat Biotechnol. 2017; 35:1179. [PubMed: 29131148]
11. Miller JB, Zhang S, Kos P, Xiong H, Zhou K, Perelman SS, Zhu H, Siegwart DJ. Angew Chem, Int Ed. 2017; 56(4):1059–1063.
12. Jiang C, Mei M, Li B, Zhu X, Zu W, Tian Y, Wang Q, Guo Y, Dong Y, Tan X. Cell Res. 2017; 27(3):440–443. [PubMed: 28117345]
13. Lee K, Conboy M, Park HM, Jiang F, Kim HJ, Dewitt MA, Mackley VA, Chang K, Rao A, Skinner C, et al. Nat Biomed Eng. 2017; 1:889. [PubMed: 29805845]
14. Wang M, Zuris JA, Meng F, Rees H, Sun S, Deng P, Han Y, Gao X, Pouli D, Wu Q, et al. Proc Natl Acad Sci U S A. 2016; 113(11):2868–2873. [PubMed: 26929348]
15. Zuris JA, Thompson DB, Shu Y, Guilinger JP, Bessen JL, Hu JH, Maeder ML, Joung JK, Chen ZY, Liu DR. Nat Biotechnol. 2015; 33(1):73–80. [PubMed: 25357182]
16. Staahl BT, Benekareddy M, Coulon-Bainier C, Banfal AA, Floor SN, Sabo JK, Urnes C, Munares GA, Ghosh A, Doudna JA. Nat Biotechnol. 2017; 35(5):431–434. [PubMed: 28191903]
17. Zincarelli C, Soltys S, Rengo G, Rabinowitz JE. Mol Ther. 2008; 16(6):1073–1080. [PubMed: 18414476]
18. Ginn SL, Alexander IE, Edelstein ML, Abedi MR, Wixon J. J Gene Med. 2013; 15(2):65–77. [PubMed: 23355455]
19. Lieber A, He CY, Meuse L, Schowalter D, Kirillova I, Winther B, Kay MA. J Virol. 1997; 71(11): 8798–8807. [PubMed: 9343240]
20. Chew WL, Tabebordbar M, Cheng JKW, Mali P, Wu EY, Ng AHM, Zhu K, Wagers AJ, Church GM. Nat Methods. 2016; 13(10):868–874. [PubMed: 27595405]
21. Fu Y, Foden JA, Khayter C, Maeder ML, Reyon D, Joung JK, Sander JD. Nat Biotechnol. 2013; 31(9):822–826. [PubMed: 23792628]
22. Kim S, Kim D, Cho SW, Kim J, Kim JS. Genome Res. 2014; 24(6):1012–1019. [PubMed: 24696461]
23. Lin S, Staahl BT, Alla RK, Doudna JA. eLife. 2014; 3:e04766. [PubMed: 25497837]
24. Sun W, Ji W, Hall JM, Hu Q, Wang C, Beisel CL, Gu Z. Angew Chem, Int Ed. 2015; 54(41): 12029–12033.
25. Lonsdale J, Thomas J, Salvatore M, Phillips R, Lo E, Shad S, Hasz R, Walters G, Garcia F, Young N, et al. Nat Genet. 2013; 45(6):580–585. [PubMed: 23715323]
26. Stockert RJ. Physiol Rev. 1995; 75(3):591–609. [PubMed: 7624395]

27. Rajeev KG, Nair JK, Jayaraman M, Charisse K, Taneja N, O'Shea J, Willoughby JLS, Yucius K, Nguyen T, Shulga-Morskaya S, et al. ChemBioChem. 2015; 16(6):903–908. [PubMed: 25786782]
28. Nair JK, Willoughby JLS, Chan A, Charisse K, Alam MR, Wang Q, Hoekstra M, Kandasamy P, Kel'in AV, Milstein S, et al. J Am Chem Soc. 2014; 136(49):16958–16961. [PubMed: 25434769]
29. Yu RZ, Graham MJ, Post N, Riney S, Zanardi T, Hall S, Burkey J, Shemesh CS, Prakash TP, Seth PP, et al. Mol Ther– Nucleic Acids. 2016; 5:e317. [PubMed: 27138177]
30. Tanowitz M, Hettrick L, Revenko A, Kinberger GA, Prakash TP, Seth PP. Nucleic Acids Res. 2017; 45(21):12388–12400. [PubMed: 29069408]
31. Chen Z, Jaafar L, Agyekum DG, Xiao H, Wade MF, Kumaran RI, Spector DL, Bao G, Porteus MH, Dynan WS, et al. Nucleic Acids Res. 2013; 41(19):e182. [PubMed: 23956220]
32. Dowdy SF. Nat Biotechnol. 2017; 35(3):222–229. [PubMed: 28244992]
33. Liu J, Gaj T, Yang Y, Wang N, Shui S, Kim S, Kanchiswamy CN, Kim J-S, Barbas CF Iii. Nat Protoc. 2015; 10(11):1842–1859. [PubMed: 26492140]
34. Sanhueza CA, Baksh MM, Thuma B, Roy MD, Dutta S, Préville C, Chrunyk BA, Beaumont K, Dullea R, Ammirati M, et al. J Am Chem Soc. 2017; 139(9):3528–3536. [PubMed: 28230359]
35. D'Souza AA, Devarajan PV. J Controlled Release. 2015; 203:126–139.
36. Li Y, Huang G, Diakur J, Wiebe LI. Curr Drug Delivery. 2008; 5(4):299–302.
37. Shulman M, Nahmias Y. Methods Mol Biol. 2013; 945:287–302. [PubMed: 23097113]
38. Liu J, Gaj T, Wallen MC, Barbas CF. Mol Ther–Nucleic Acids. 2015; 4:e232. [PubMed: 25756962]
39. Appelbaum JS, LaRochelle JR, Smith BA, Balkin DM, Holub JM, Schepartz A. Chem Biol. 2012; 19(7):819–830. [PubMed: 22840770]
40. Oakes BL, Nadler DC, Flamholz A, Fellmann C, Staahl BT, Doudna JA, Savage DF. Nat Biotechnol. 2016; 34(6):646–651. [PubMed: 27136077]
41. Lee YC, Townsend RR, Hardy MR, Lönngren J, Arnarp J, Haraldsson M, Lönn H. J Biol Chem. 1983; 258(1):199–202. [PubMed: 6848494]
42. Khorev O, Stokmaier D, Schwardt O, Cutting B, Ernst B. Bioorg Med Chem. 2008; 16(9):5216–5231. [PubMed: 18358727]
43. Varkouhi AK, Scholte M, Storm G, Haisma HJ. J Controlled Release. 2011; 151(3):220–228.
44. Shete HK, Prabhu RH, Patravale VB. J Nanosci Nanotechnol. 2014; 14(1):460–474. [PubMed: 24730275]
45. Liang, W., Lam, JKW. Endosomal Escape Pathways for Non-Viral Nucleic Acid Delivery Systems. In: Cesera, B., editor. Molecular Regulation of Endocytosis. Intech; 2012. p. 429-456.
46. Rittner K, Benavente A, Bompard-Sorlet A, Heitz F, Divita G, Brasseur R, Jacobs E. Mol Ther. 2002; 5(2):104–114. [PubMed: 11829517]
47. This profile was also qualitatively observed for the pair Cas9-2lig-AFr-1NLS and Cas9-AFr-1NLS RNPs; see Figure S16B.
48. Dai W-J, Zhu L-Y, Yan Z-Y, Xu Y, Wang Q-L, Lu X-J. Mol Ther–Nucleic Acids. 2016; 5:e349. [PubMed: 28131272]
49. Chew WL. Wiley Interdiscip Rev Syst Biol Med. 2018; 10(1):e1408.

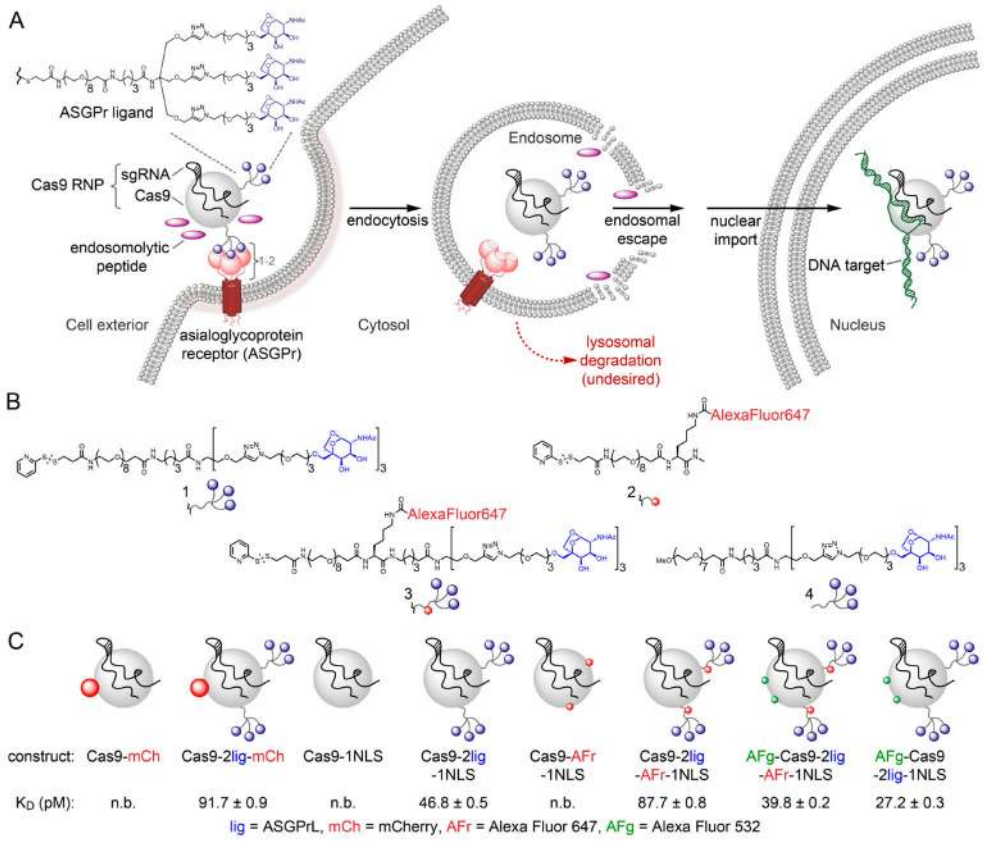

Figure 1.

(A) Receptor-facilitated, cell-selective gene editing. Schematic representation of Cas9-ASGPrL RNP and its transit from the extracellular medium to the nucleus. (B) Pyridyl disulfide ASGPr ligand and/or fluorophore precursors **1**–**3** and competing ligand **4** used in this study. (C) Legend of constructs used in this study, with corresponding ASGPr-binding affinities for various RNPs measured using SPR; reported values are from three replicates (standard error is reported); n.b.: no binding (top concentration tested = 10 nM). RNP made using sgRNA targeting EMX1.

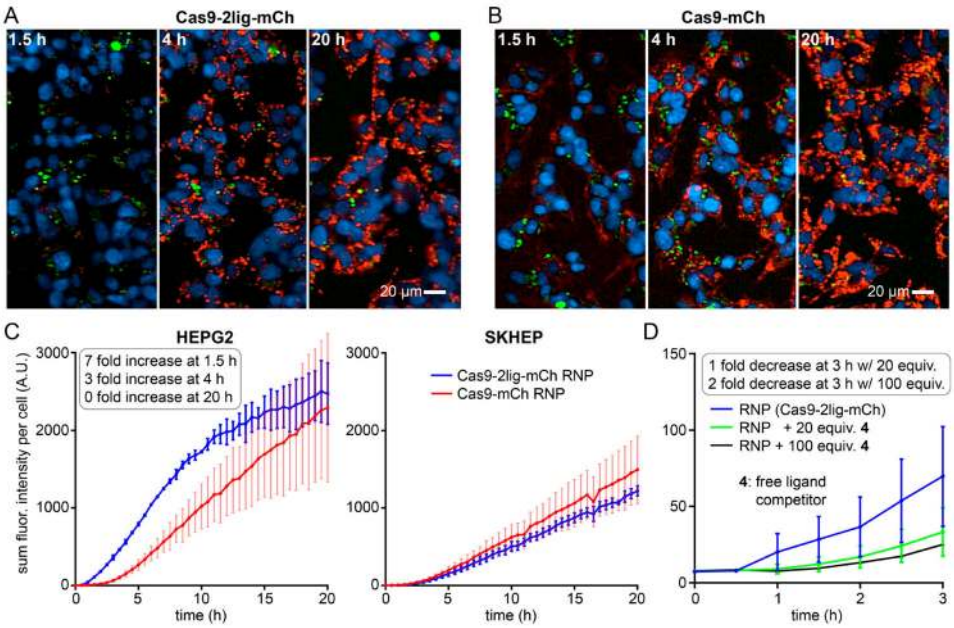

Figure 2.

Internalization in HEPG2 cells (ASGPr+) of Cas9-2lig-mCh (A) and Cas9-mCh (B) RNPs observed by live cell imaging at 1.5, 4, and 20 h; 20 h image contrast was adjusted down for clarity. Blue: Hoechst stain of cell nuclei. Green: Endolysosomal compartment stained using dextran488. Red: Intracellular Cas9 visualized via mCherry fluorescence. (C) Quantification of intracellular RNP accumulation in HEPG2 and SKHEP cells over 20 h. (D) Ligand competition experiment in HEPG2 cells with Cas9-2lig-mCh RNP and competing ASGPr ligand **4** (see the Supporting Information for more details). Fluorescence intensity was quantified using the sum of spots per cell (mean per well), reported as AU (absorbance units). Each data point (C,D) represents three technical replicate wells with a minimum of 10000 cells quantified per well. For (C) and (D), arithmetic means and standard deviations of the mean were calculated and plotted using GraphPad Prism version 7.02. Corresponding RNPs made from sgRNA targeting EMX1.

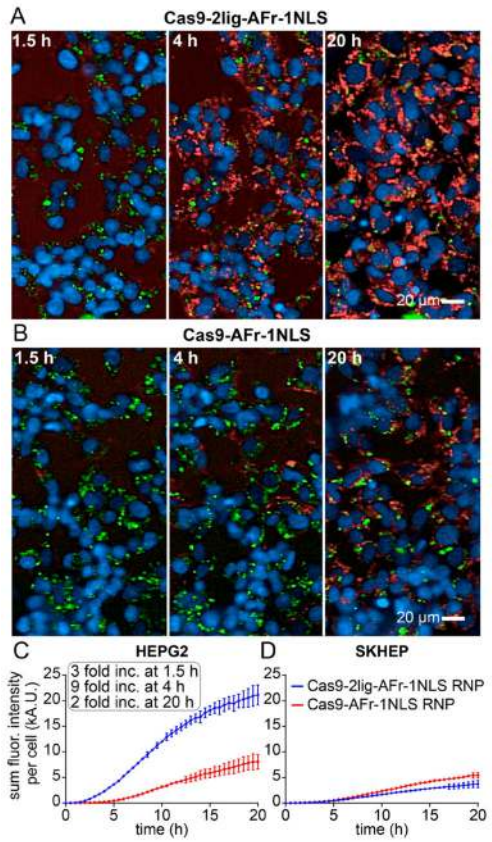

Figure 3.

Internalization in HEPG2 cells (ASGPr+) of Cas9-2lig-AFr-1NLS (A) and Cas9-AFr-1NLS (B) RNPs observed by live cell imaging at 1.5, 4, and 20 h; 20 h images contrast was adjusted down for clarity. Blue: Hoechst stain of cell nuclei. Green: Endolysosomal compartment stained using dextran488. Red: Intracellular Cas9 visualized via AF647 fluorescence. (C) Quantification of intracellular RNP accumulation in HEPG2 cells over 20 h. (D) Quantification of intracellular RNP accumulation in SKHEP cells over 20 h. Fluorescence intensity was quantified using the sum of spots per cell (mean per well), reported as kA.U (10^3 absorbance units). Each data point (C, D) represents three technical replicate wells, with a minimum of 10000 cells quantified per well. For (C) and (D), arithmetic means and standard deviations of the mean were calculated and plotted using GraphPad Prism version 7.02. Corresponding RNPs made from sgRNA targeting EMX1.

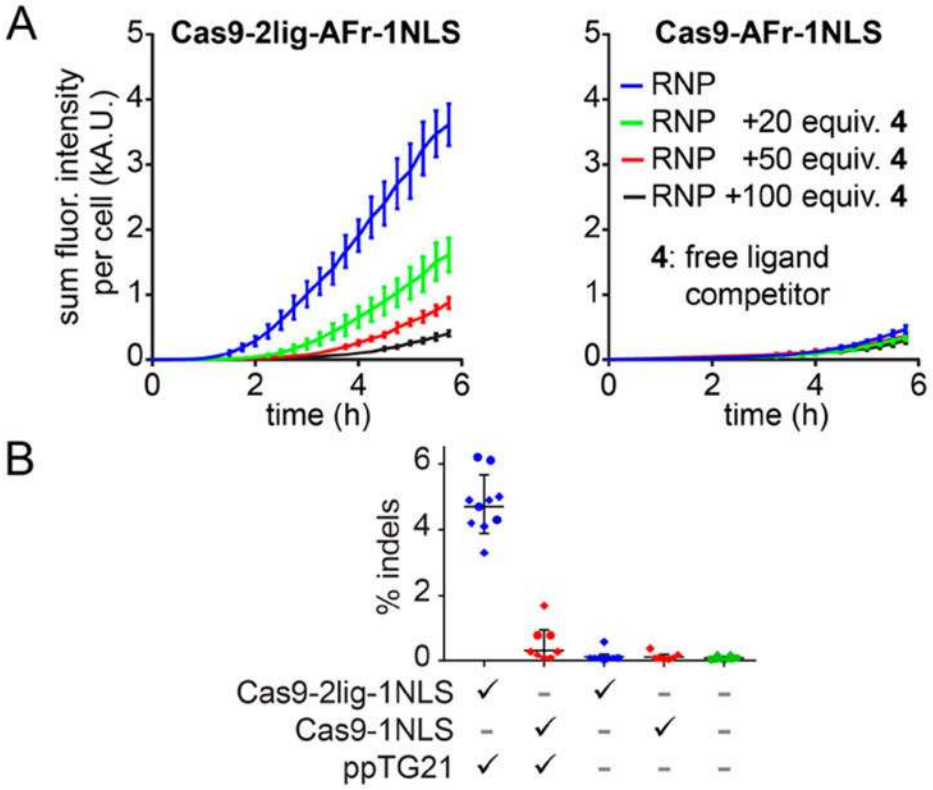

Figure 4.

Receptor-mediated uptake and genome editing. (A) Ligand competition experiment in HEPG2 cells (ASGPr+) with Cas9-2lig-AFr-1NLS RNP or Cas9-AFr-1NLS RNP using competing ASGPr ligand **4** (see the Supporting Information for more details). Fluorescence intensity was quantified using the sum of spots per cell (mean per well), reported as kA.U (10^3 absorbance units). Each data point represents three technical replicate wells, with a minimum of 10000 cells quantified per well. Arithmetic means and standard deviations of the mean were calculated and plotted using GraphPad Prism version 7.02. Corresponding RNPs made from sgRNA targeting EMX1. (B) Receptor-facilitated gene editing with Cas9-2lig-1NLS vs Cas9-1NLS RNP. Percentage indel rates derived from deep sequencing (n = 7–10 replicates; see also Table S1). Blue points represent samples treated with Cas9-2lig-1NLS, red points represent samples treated with Cas9–1NLS and green represents untreated controls. Diamonds represent assays done at Pfizer (Groton, CT) and circles represent assays done at UC Berkeley. The midpoint bars depict the geometric mean and the error bars depict the geometric standard deviation. The image was generated using Graphpad Prism© version 7.02. The corresponding RNPs were made from sgRNA targeting EMX1.